HHS Public Access

Author manuscript

Oncogene. Author manuscript; available in PMC 2017 March 03.

Published in final edited form as:

Oncogene. 2017 March 02; 36(9): 1232–1244. doi:10.1038/onc.2016.288.

Yes-Associated Protein Mediates Immune Reprogramming in Pancreatic Ductal Adenocarcinoma

Shigekazu Murakami[1,*], **David Shahbazian**[1,*], **Rishi Surana**[1,*], **Weiying Zhang**[1,#], **Hengye Chen**[1], **Garrett T. Graham**[1], **Shannon M. White**[1], **Louis M. Weiner**[1], and **Chunling Yi**[1,2]

[1]Lombardi Comprehensive Cancer Center, Georgetown University Medical Center, Washington, DC 20057, USA

Abstract

Pancreatic ductal adenocarcinoma (PDAC) is characterized by a high degree of inflammation and profound immune suppression. Here we identify Yes-associated protein (Yap) as a critical regulator of the immunosuppressive microenvironment in both mouse and human PDAC. Within *Kras:p53* mutant pancreatic ductal cells, Yap drives the expression and secretion of multiple cytokines/chemokines, which in turn promote the differentiation and accumulation of Myeloid-derived suppressor cells (MDSCs) both *in vitro* and *in vivo*. Pancreas-specific knockout of *Yap* or antibody-mediated depletion of MDSCs promoted macrophage reprogramming, reactivation of T cells, apoptosis of *Kras* mutant neoplastic ductal cells, and pancreatic regeneration after acute pancreatitis. In primary human PDAC, YAP expression levels strongly correlate with a MDSC gene signature, and high expression of YAP or MDSC-related genes predicts decreased survival in PDAC patients. These results reveal multifaceted roles YAP in PDAC pathogenesis and underscore its promise as a therapeutic target for this deadly disease.

Keywords

YAP; PDAC; T cells; inflammation; MDSC; Macrophages; acute pancreatitis

Pancreatic ductal adenocarcinoma (PDAC) is a devastating malignancy that accounts for approximately 48,000 new diagnoses and 40,000 deaths in the United States each year (Siegel et al 2015). PDAC is commonly diagnosed at an advanced stage and has a five-year survival rate of less than 2% (Siegel et al 2015). Precursor lesions, termed pancreatic intraepithelial neoplasia (PanIN), are graded 1–3 with PanIN3 characterized by disorganized growth and prominent nuclear atypia (Hruban et al 2001). It is hypothesized that trans-differentiation of acinar cells to duct-like cells, a process termed acinar to ductal metaplasia (ADM), is an initiating event in the development of PanIN. Virtually all PanIN lesions and invasive PDAC involve activating mutations in *KRAS*. Additional inactivating mutations of tumor suppressor *CDKN2A, TP53* or *SMAD4* occur commonly in late stage PanINs and

[2]Corresponding author. cy232@georgetown.edu.
[*]These authors contributed equally to this manuscript.
[#]Present address: Department of Cancer Research, College of Life Sciences, Nankai University, Tianjin, P.R. China.

PDAC and are associated with a higher metastatic burden (Bardeesy et al 2001, Jaffee et al 2002, Ryan et al 2014, Schutte et al 1997). Various genetically engineered mouse models have been developed to reproduce the progression of human PDAC (Aguirre et al 2003, Brembeck et al 2003, Grippo et al 2003, Hingorani et al 2003, Tuveson et al 2006). The model that best mimics the progression of human PDAC involves expression of a mutant *Kras* ($Kras^{G12D}$) from the endogenous *Kras* locus through a Cre recombinase that is under control of the pancreas-specific promoter *p48* (from now on referred to as the KC model) (Hingorani et al 2005). These animals develop ADM with the full spectrum of PanIN lesions that eventually progress to frank PDAC. Concomitant expression of mutated p53 ($Trp53^{R172H}$) with $Kras^{G12D}$ (from now on referred to as the KPC model) accelerates development of precursor lesions and progression to invasive PDAC (Hingorani et al 2005).

The tumor microenvironment of both human and mouse PDAC is characterized by marked desmoplasia and a prominent cellular infiltrate predominantly composed of fibroblasts, leukocytes and endothelial cells (Feig et al 2012). In spite of the presence of tumor infiltrating leukocytes (TILs) at variable levels, the vast majority of PDAC tumors exhibit profound immune dysfunction due to the recruitment of immune-suppressive leukocytes such as myeloid-derived suppressor cells (MDSCs) and tumor-associated macrophages (TAMs) (Bayne et al 2012, Clark et al 2007, Khaled et al 2014, Kurahara et al 2013, Porembka et al 2012, Pylayeva-Gupta et al 2012, Zeng et al 2014, Zhao et al 2009). Once recruited to the tumor microenvironment, MDSCs and TAMs directly suppress T-cell function by depleting amino acids critical for T-cell activation and proliferation, by producing nitric oxide (NO) and reactive oxygen species (ROS) that suppress T-cell intracellular signaling, and by downregulating selectins required for T-cell homing to lymph nodes (Parker et al 2015). MDSCs and TAMs also indirectly inhibit T-cell activity by secreting suppressive cytokines/chemokines (such as IL-6, IL-10 and TGF-β) which induce regulatory T-cells (T_{reg}) and inhibit the ability of antigen-presenting cells (APCs) to activate T cells (Parker et al 2015). In PDAC, the massive recruitment of MDSCs and TAMs has also been identified as a potential underlying cause for the relative unresponsiveness of PDAC to T-cell checkpoint inhibitors (Bayne et al 2012, Lu et al 2011, Pylayeva-Gupta et al 2012, Stromnes et al 2014, Zhu et al 2014).

We previously identified Yes-associated protein (YAP), a transcriptional coactivator of the TEAD family of transcription factors, as a crucial driver of proliferation in *KRAS* mutant neoplastic pancreatic ductal cells (Zhang et al 2014). We demonstrated that pancreas-specific deletion of *Yap* in KC and KPC mice completely blocked progression of ADM/PanIN1 into PDAC, resulting in 100% PDAC-free survival (Zhang et al 2014). Subsequent studies showed that YAP could also substitute oncogenic KRAS in promoting the growth of PDAC tumors as well as lung adenocarcinomas (Kapoor et al 2014, Shao et al 2014), and confer resistance to MAPK pathway inhibitors in *KRAS* or *BRAF* mutant tumor cells (Hugo et al 2015, Kim et al 2015, Lin et al 2015).

Pancreatitis (acute or chronic) is an inflammatory disease of the pancreas, which has been linked to increased risks of developing PDAC in humans (Lowenfels et al 1993, Munigala et al 2014, Ryan et al 2014). Acute pancreatitis can be induced in mice with repeated injections of a cholecystokinin receptor agonist, caerulein. In response to caerulein treatment, wildtype

(WT) pancreata undergo transient ADM, inflammation and parenchymal apoptosis, but quickly regenerate (Jensen et al 2005). In contrast, ADM and inflammation persist in *Kras* mutant pancreata after caerulein-induced acute pancreatitis, resulting in accelerated PDAC onset (Carriere et al 2009, Carriere et al 2011, Morris et al 2010). Our previous study showed that inhibition of *YAP* blocked the expression of multiple secreted factors including IL-6, IL-1α, COX2, MMP7, CTGF and CYR61 by tumor cells, and decreased leukocyte recruitment and desmoplasia (Zhang et al 2014). These data suggest that YAP and a YAP-controlled secretome promote the progression of *KRAS* mutant early precursor lesions to PDAC at least in part by modulating the composition of the tumor microenvironment. Here, we utilize the well-established murine acute pancreatitis model to reveal a novel cancer cell non-autonomous function for YAP in modulating the immune program elicited by oncogenic *Kras* during the development of PDAC. Our results suggest that YAP acts as a transcriptional driver of cytokines that orchestrate the immune suppressive microenvironment within PDAC.

RESULTS

Yap ablation resolves inflammation and causes regeneration of *Kras:Trp53* mutant pancreata following acute pancreatitis

Following a well-established protocol of two consecutive days of caerulein injections (Jensen et al 2005), acute pancreatitis was induced in *p48-Cre* (Cre), $Yap^{flox/flox}$;*p48-Cre* (Yap^{KO}), *LSL-*$Kras^{G12V}$;*LSL-*$p53^{R172H}$;*p48-Cre* (KPC) and *LSL-*$Kras^{G12V}$;*LSL-*$p53^{R172H}$;$Yap^{flox/flox}$;*p48-Cre* (KPYC) mice at 8 weeks of age when pancreata from all genotypes were histologically normal prior to induction of pancreatitis. Similar to previously described results from WT mice (Jensen et al 2005), both Cre and Yap^{KO} pancreata displayed transient formation of ADM characterized by $Ck19^+$ ductal structures and associated infiltration of $Vimentin^+$ stromal cells at 48 hours post-caerulein injection. These histological changes were largely resolved by one-week post-injection (Supplementary Fig. 1a). In contrast, ADM and associated desmoplasia, including infiltrates of αSma^+ fibroblasts and $CD45^+$ leukocytes, remained prevalent at one week post-injection in both KPC and KPYC pancreata (Fig. 1a–1b). By 5 weeks post-injection, however, KPYC pancreata recovered to nearly normal histological appearance with only remnant Ck19, Vimentin, αSma and CD45 staining, whereas persistent inflammation and progression of ADM to early stage PanINs were evident in KPC pancreata (Fig. 1a–1b). While KPC mice started to succumb to PDAC by 9 weeks after caerulein-induced acute pancreatitis, KPYC mice remained PDAC free with fully regenerated pancreata (Supplementary Fig. 1b). These findings suggest that while Yap is not required for initiating ADM and inflammation in response to caerulein, its activity is indispensable for sustaining extended inflammation and preventing regeneration in *Kras:Trp53* mutant pancreata.

Deletion of *Yap* reactivates T cells and promotes apoptosis of *Kras:Trp53* mutant neoplastic ducts following acute pancreatitis

Parenchymal apoptosis is a necessary step that precedes pancreatic regeneration following acute pancreatitis (Bhatia 2004). We found that at one week post caerulein injection, KPYC but not KPC pancreata exhibited robust cleaved-Caspase 3 staining, particularly within

regions of ADM (Fig. 2a). We previously showed that *Yap* ablation alone did not induce apoptosis in *Kras:Trp53* mutant pancreatic ductal cells (Zhang et al 2014), suggesting that Yap prevented apoptosis in KPC pancreata following acute pancreatitis possibly by modulating the inflammatory response.

Given the well-established function of T cells in inducing target cell apoptosis, we examined the percentage of $CD3^+$ T cells among the infiltrating $CD45^+$ leukocytes in KPC and KPYC pancreata. In situ immunohistochemistry (IHC) as well as *ex vivo* flow cytometry analysis demonstrated that infiltrating T cells were abundant in both KPC and KPYC pancreata at one week after caerulein treatment, the total numbers of T cells and the ratio of $CD4^+$ T-helper (Th) to $CD8^+$ cytotoxic T lymphocytes (CTLs), and the percentage of $FoxP3^+CD4^+$ Treg cells were also comparable between the two groups (Fig. 2a–2d, and Supplementary Fig. 2a). Despite the similarities in overall numbers of infiltrating T cells, we found that KPYC pancreata contained significantly increased levels of cytokines associated with T-cell activation, including Ifnγ, Il-2, Il-15, Il-4 and Il-13, compared to KPC or WT pancreata (Supplementary Fig. 3a). To further characterize the recruited T cells, we performed co-staining of CD3 with CD44 (surface marker for antigen activated T cells) or Granzyme B (GzmB, a serine proteinase expressed and secreted by activated T cells), which revealed the presence of a significantly higher percentage of $CD3^+CD44^+$ and $CD3^+GzmB^+$ cells within KPYC pancreata compared to KPC pancreata (Fig. 2a). As CTLs are thought to be the primary mediator of anti-tumor immunity, we isolated CTLs from both KPC and KPYC pancreata and investigated expression of molecules associated with CTL activation. Quantitative real-time PCR (qRT-PCR) analysis showed that $CD45^+CD3^+CD8^+$ CTLs purified from KPYC pancreata exhibited significantly higher expression of activation markers *Prf1, Gzmb* as well as the proliferation marker *Pcna*, compared to those from KPC pancreata (Fig. 2e). Consistent with increased T cell activation, KPYC pancreata exhibited elevated expression of genes involved in T cell receptor (TCR) signaling compared to KPC pancreata (Fig. 2f, and Supplementary Fig. 2b), albeit the overall transcriptional profiles were largely indistinguishable between the KPC and KPYC pancreata at this time point (Supplementary Fig. 2c). These results suggest that Yap is responsible for preventing T cell activation by *Kras:Trp53* mutant neoplastic ductal cells, allowing the survival of *Kras:Trp53* mutant neoplastic ductal cells.

Yap inactivation enhances infiltration of MHCII+ macrophages in *Kras:Trp53* mutant pancreata following acute pancreatitis

As antigen presentation is an essential step in T cell activation, we next examined the expression of major histocompatibility class II (MHCII) molecules, which are predominantly expressed on the surface of antigen presenting cells (APCs) including dendritic cells, B cells and macrophages. IHC analysis showed a significant increase in the total number of $MHCII^+$ cells in the pancreata of KPYC mice compared to KPC mice at one week post caerulein injection (Fig. 3a). Moreover, $MHCII^+$ cells were present throughout the entire pancreas and in close proximity to $CD3^+$ T cells in KPYC pancreata, whereas they were mostly concentrated in the periphery of the pancreas and rarely in contact with $CD3^+$ T cells in KPC pancreata (Fig. 3a). We observed a significant increase in the total number of $F4/80^+$ macrophages as well as an increase in the proportion of $F4/80^+$ macrophages that

express MHCII in KPYC pancreata compared to KPC pancreata (Fig. 3a–3c, and Supplementary Fig. 4a–4b). In contrast, there were no significant changes in the recruitment of $CD19^{+}MHCII^{+}$ B-cells or $CD11c^{+}MHCII^{+}$ dendritic cells (Fig. 3d–3e, Supplementary Fig. 5 and 6). Notably, $F4/80^{+}$ macrophages in KPYC animals were distributed throughout the pancreatic parenchyma and localized to areas of MHCII expression as demonstrated by IHC (Fig. 3a). The macrophages isolated from KPYC pancreata also expressed more iNos (*Nos2*) and lower levels of Arginase (*Arg*) compared to those from KPC pancreata, suggesting that macrophages adopted a more anti-tumorigenic phenotype in KPYC pancreata, while the phenotype of KPC macrophages were primarily tumor-promoting (Fig. 3f) (Clark et al 2007).

Yap inactivation blocks accumulation of MDSCs in the spleens and pancreata of *Kras:Trp53* mutant mice following acute pancreatitis

$Gr1^{+}CD11b^{+}$ MDSCs have been identified in a series of studies as a major immune suppressive cell population within KPC PDAC tumors that are capable of suppressing T cell activity both *in vitro* and *in vivo* (Bayne et al 2012, Clark et al 2007, Porembka et al 2012, Pylayeva-Gupta et al 2012, Zhao et al 2009). Therefore, we investigated how *Yap* ablation affected the recruitment of MDSCs in *Kras:Trp53* mutant pancreata following caerulein-induced acute pancreatitis. Interestingly, there were significantly fewer $Gr1^{+}CD11b^{+}$ MDSCs both in the spleen and pancreas of KPYC animals compared to KPC animals (Fig. 4a–4b). In mice, MDSCs can be further divided into two functionally distinct subtypes based on differential expression of Ly6G and Ly6C antigens, both of which are recognized by the Gr1 antibody. Granulocytic MDSC (G-MDSC) express Ly6G and are Ly6C negative, while monocytic MDSC (M-MDSC) are negative for Ly6G and express Ly6C (Parker et al 2015). IHC analysis using Ly6G and Ly6C specific antibodies demonstrated that both G-MDSC and M-MDSC populations were decreased in KPYC pancreata compared to KPC pancreata (Fig. 4c). These results indicate that Yap is necessary for mutant Kras-induced systematic accumulation of MDSCs following caerulein-induced acute pancreatitis.

Yap is required for the expression of secreted factors that induce differentiation of bone marrow myeloid progenitor cells into MDSCs by *Kras:Trp53* mutant PDAC cells

MDSCs are generated in the bone marrow from myeloid progenitors in response to tumor-derived factors such as colony stimulating factors (CSFs), IL-6, IL-1β, prostaglandin E2 (PGE2), tumor necrosis factor α (TNFα) and vascular endothelial growth factor (VEGF) (Katoh and Watanabe 2015, Parker et al 2015). Previous studies demonstrated that conditioned media (CM) from KPC PDAC cells were able to induce differentiation of myeloid progenitor cells into functional MDSCs capable of suppressing T cells (Bayne et al 2012, Pylayeva-Gupta et al 2012).

To examine whether Yap drives the expression of MDSC-polarizing factors by KPC tumor cells, we incubated bone marrow isolated from WT animals with conditioned media (CM) from KPYC cells transduced with either vector control or Flag-Yap (Zhang et al 2014). As shown in Fig. 4d, reconstitution of Yap in KPYC tumor cells rescued the ability of these cells to drive differentiation of the bone-marrow-derived myeloid progenitor cells into MDSCs. Of note, CM from Yap re-expressing KPYC cells did not affect the survival of

differentiated MDSCs or induce differentiation of MDSC into macrophages or dendritic cells (Supplementary Fig. 7a–7b). To confirm Yap's role in mediating the expression of MDSC-polarizing factors, we generated KPC tumor-derived PDAC cell lines stably transduced with either a control empty lentiviral vector (pTRIPZ) or a lentiviral vector expressing Yap shRNA (pTRIPZ-Yapsh) in a doxycycline-inducible system (Supplementary Fig. 7c). Incubation of WT bone marrow with CM from either control or Yap-knockdown (YapKD) KPC cells showed that silencing of Yap blocked the ability of KPC tumor cells to drive MDSC polarization from bone-marrow-derived myeloid progenitor cells (Supplementary Fig. 7d). These results suggest that Yap mediates the expression of soluble factors that promote MDSC polarization by KPC tumor cells.

Yap drives the transcription of MDSC-polarizing cytokines in *Kras:Trp53* mutant pancreatic ductal cells

To identify Yap-regulated secreted factors that are responsible for inducing MDSC polarization, we conducted cytokine/chemokine profiling of the pancreata of WT, KPC and KPYC animals at one week post caerulein challenge. Among the cytokines that have previously been implicated in MDSC differentiation and/or recruitment (Parker et al 2015), we detected a significant upregulation of Il-6 (*Il6)*, GM-Csf (*Csf2*), G-Csf (*Csf3*), M-Csf (*Csf1*), Tnfα, Il-3, Kc (Cxcl1), Mip-2 (Cxcl2), and Mcp-1 (Ccl2) in KPC pancreata compared to WT control, whereas KPYC pancreata maintained similar levels of the above-mentioned cytokines as those of WT animals (Fig. 5a and Supplementary Fig. 3b). In contrast, both KPC and KPYC pancreata expressed significantly higher levels of Il-1α and Il-9 compared to WT pancreata (Supplementary Fig. 3c), while other cytokines such as Il-1β and Il-12 were not significantly changed in either KPC or KPYC pancreata compared to WT control (Supplementary Fig. 3d).

Multiple cell types within PDAC tumors could be responsible for the expression and secretion of above-mentioned cytokines/chemokines. To determine which cytokines/chemokines were directly secreted by the tumor cells in a Yap-dependent fashion, we carried out cytokine/chemokine profiling of CM from KPC tumor cells carrying inducible Yap shRNA or an empty vector control (Supplementary Fig. 7c). Notably, doxycycline-induced knockdown of Yap specifically reduced the levels of secreted Il-6, G-Csf and M-Csf compared to vector control (Fig. 5b), while the other cytokines/chemokines included in our analysis were not affected (not shown). This finding was corroborated by re-expression of Yap in KPYC cells, which caused a significant increase in *Il6, Csf1, Csf2 and Csf3* mRNA levels and in the concentrations of Il-6, G-Csf and M-Csf that were secreted into the medium (Fig. 5c–5d).

Yap partners with the Tead/Tef family transcription factors to activate target gene expression. *In silico* analysis identified several Tead-binding consensus sites within the promoter sequences of the above-mentioned pro-MDSC cytokines. Chromatin immunoprecipitation (ChIP) analysis confirmed that in *Kras:Trp53* mutant PDAC cells, endogenous Yap was enriched on the promoter regions of *Il6* and *Csf1-3* that contained Tead binding sites but not in the 3'UTR regions that lacked Tead binding motifs (Fig. 5e). Similar results were obtained using Flag antibodies in KPYC cells reconstituted with empty vector or Flag-

tagged Yap (Fig. 5f). Taken together, our data indicate that *Il6* and *Csf1-3* are transcriptionally controlled by the Yap/Tead complex in *Kras:p53* mutant pancreatic ductal cells.

Depletion of MDSCs reactivates T cells and promotes tissue regeneration in *Kras:Trp53* mutant pancreata following acute pancreatitis

Finally, we investigated whether accumulation of MDSCs was indeed responsible for preventing pancreatic recovery in *Kras* mutant animals following acute pancreatitis. 8-week-old *LSL-Kras^{G12V};p48-Cre* (KC) mice were first subjected to two consecutive days of caerulein injections, and then treated with either control IgG or αGr1 antibodies over the course of two weeks (Fig. 6a). Treatment with αGr1 antibodies but not IgG control induced a variable degree of pancreatic recovery in KC mice (Fig. 6b). Importantly, the extent of recovery inversely correlated with levels of remaining MDSCs in the pancreas (Fig. 6b). Depletion of MDSCs also led to influx of MHCII$^+$ cells, many of which were in close contact with CD3$^+$ T cells (Fig. 6b). These results demonstrate that MDSCs limit both pancreatic recovery and accumulation of MHCII$^+$ cells within the pancreas following caerulein–induced acute pancreatitis.

High YAP expression levels correlate with high expression of MDSC-related genes and poor survival in human PDAC

To assess the clinical relevance of our finding, we analyzed The Cancer Genome Atlas (TCGA) RNAseq dataset containing 178 human PDAC samples. First, we performed unsupervised clustering of the patient samples using a group of 40 genes that have been previously linked to MDSC generation, recruitment or function, which segregated the patients into three major groups (Fig. 7a). As shown in Fig. 7b, the patients classified as having a “high” MDSC gene expression profile expressed significantly higher levels of YAP compared to those with a “low” MDSC classification, implying that YAP may also drive MDSC recruitment in PDAC patients.

Consistent with previous reports (Gabitass et al 2011, Markowitz et al 2015), we found that patients whose tumors exhibited a “high” MDSC-related gene expression profile survived a significantly shorter time than the patients with a “low” MDSC profile (Fig. 7c). Given the strong correlation between MDSC status and YAP expression, we stratified the same set of TCGA patient samples into three groups based on YAP expression levels. Similar to the MDSC gene signature, higher YAP expression levels strongly correlated with poorer overall survival in PDAC patients (Fig. 7d). While these results do not indicate a causative relationship, they support the potential clinical applicability of our finding that Yap acts as an important driver of MDSC-mobilizing cytokines/chemokines in a mouse model of PDAC.

DISCUSSION

Abundant infiltration of immunosuppressive leukocytes such as MDSCs and TAMs is an early event during PDAC oncogenesis and plays a key role in restraining anti-tumor immunity (Clark et al 2007). Here we show that the immunosuppressive microenvironment orchestrated by *Kras* mutant neoplastic ductal cells following induction of acute pancreatitis

depends on the transcription regulator Yap. Ablation of *Yap* in *Kras:Trp53* mutant pancreatic epithelial cells circumvented recruitment of MDSCs in favor of $MHCII^+$ anti-tumor macrophages, resulting in reactivation of T lymphocytes, apoptosis of neoplastic ductal cells, and tissue regeneration following acute pancreatitis (Fig. 8). Mechanistically, we show that Yap binds to the promoter regions of *Il6* and the *Csfs* and controls their transcription in *Kras:Trp53* mutant PDAC cells. In the absence of Yap, *Kras:Trp53* mutant PDAC cells were unable to produce Il-6 and the Csfs and failed to induce MDSC polarization *in vitro* and recruitment *in vivo*. Notably, besides blockade of Il-6 and Csfs, *in vivo* abrogation of *Yap* also caused accruement of cytokines known to promote T-cell activity (including Ifnγ, Il-2, Il-15, Il-4 and Il-13), while abolishing Kras-induced upregulation of Tgf-β1, Tgf-β2, Il-3 and Lif. Whereas it remains unresolved how Yap regulates the *in vivo* expression of these cytokines, our data suggest that Yap functions as a key determinant of the oncogenic-Kras driven inflammatory program that supports the progression of precursor lesions to frank PDAC.

Since its discovery 20 years ago, YAP has been established as an important cell-intrinsic regulator of proliferation, survival and differentiation in response to various environmental cues (Plouffe et al 2015). Here we demonstrate that Yap also acts extrinsically on the tumor microenvironment as a critical immune regulator in *Kras* mutant pancreata. Importantly, ablation of *Yap* alone did not alter the normal kinetics of caerulein-induced acute pancreatitis under WT background. In *Kras:Trp53* mutant pancreata, *Yap* knockout also did not prevent prolonged inflammation and the accompanied global changes in transcription, nor did it completely reverse all the cytokines induced by oncogenic Kras. These results suggest that Yap does not simply function as a general inflammatory promoter, but rather controls the secretion of a distinct subset of oncogenic Kras-induced tumor-promoting cytokines.

Our current study identifies Yap-dependent robust upregulation of secreted Il-6, G-Csf, GM-Csf, M-Csf, Tnfα, and Il-3 in KPC pancreata. Our previous data demonstrated that Yap is required for both *in vitro* and *in vivo* expression of Cox2, an enzyme that mediates PGE2 synthesis (Zhang et al 2014). All of these cytokines have been previously established as critical mediators of MDSC polarization (Bayne et al 2012, Lechner et al 2010, Mace et al 2013, Marigo et al 2010, Obermajer et al 2011, Obermajer et al 2012, Phan et al 2013, Pylayeva-Gupta et al 2012, Sinha et al 2007, Sinha et al 2008, Strauss et al 2015, Stromnes et al 2014, Zhang et al 2009, Zhao et al 2012, Zhu et al 2014), suggesting that these cytokines likely function in concert to promote MDSC differentiation under the direction of Yap. In addition to regulating the above-mentioned MDSC-polarizing cytokines, we found that *in vivo* deletion of *Yap* in *Kras:Trp53* mutant pancreatic epithelial cells abrogated the accumulation of several MDSC-attracting cytokines including Kc (Cxcl1), Mip2 (Cxcl2), and Mcp-1 (Ccl2) in the pancreas (Acharyya et al 2012, Tsou et al 2007). Interestingly, a recent study showed that YAP mediates the expression of CXCL5 by prostate tumor cells, which is responsible for attracting MDSCs to the tumor site (Wang et al 2016). Thus, Yap-mediated tumor secretomes may not only affect MDSC differentiation from myeloid progenitor cells, but also promote their recruitment to the tumor microenvironment (Fig. 8).

Like MDSCs, TAMs can also suppress productive anti-tumor immunity and have been associated with a poor prognosis in many types of cancer, including PDAC (Noy and Pollard 2014). We found that the dramatic decrease in the MDSC population in KPYC pancreata was accompanied by a reciprocal increase in the percentage of $MHCII^{+}F4/80^{+}$ macrophages. Not only did the overall numbers of $MHCII^{+}F4/80^{+}$ macrophages increase significantly in KPYC pancreata, they also exhibited enhanced tissue infiltration, increased contact with $CD3^{+}$ T cells, and increased expression of iNos2 with a concomitant decrease in Arginase expression suggesting that deletion of *Yap* induced reprograming of TAMs from a tumor-promoting to tumor-suppressing phenotype. Interestingly, the effects of *Yap* ablation on TAMs are reminiscent of that of Csf1/Csf1R blockade, which caused similar skewing of $MHCII^{low}$ to $MHCII^{high}$ macrophages and bolstered antitumor T-cell responses (Mok et al 2014, Zhu et al 2014). These data suggest that Yap may promote recruitment of MDSC and tumor-promoting TAM in part by activating Csf1R signaling.

It remains to be determined how Yap ablation causes concomitant accumulation of $MHCII^{+}F4/80^{+}$ cell population while decreasing MDSC recruitment, considering that many of the Yap-controlled cytokines such as Csfs, Il-6, and Ccl2 drive the differentiation and recruitment of both MDSC and macrophages (Falk and Vogel 1988, Kitamura et al 2015, Lacey et al 2012, Li et al 2015, Roca et al 2009, Sierra-Filardi et al 2014). A recent study has shown that during prolonged pancreatitis, IL-4/IL-13 signaling drives alternatively activation of macrophages at least in part by promoting the proliferation of either tissue resident macrophages or recruited monocytes that differentiated to macrophage (Xue et al 2015). In support of this scenario, we find that KPYC pancreata exhibit increased Il-4 and Il-13 expression compared to KPC pancreata at one-week post caerulein treatment. Besides Il-4 and Il13, KPYC pancreata also express elevated Mip-1a (Ccl3) and Il-7 compared to KPC pancreata. Interestingly, both Mip-1a and Il-7 have been previously shown to stimulate macrophage maturation/tumoricidal activity (Alderson et al 1991, Fahey et al 1992, Lindell et al 2001). Therefore, it would be interesting in the future to elucidate the mechanisms by which Yap modulates the expression of Il-4, Il-7, Il-13 and Mip-1a (Ccl3), and determine which factor(s) are responsible for driving the macrophage re-activation in KPYC pancreata.

Given the rapidly accumulating evidence supporting the critical importance of YAP in many types of human cancer, efforts are underway to develop therapeutic inhibitors against YAP (Johnson and Halder 2014). In agreement with our results from the mouse model, we find that YAP expression levels strongly correlate with those of MDSC signature genes and both high YAP levels and high expression of MDSC-related genes predict poor survival in PDAC patients. These result suggest that successful blockade of YAP in pancreatic cancer has the potential to not only inhibit tumor cell proliferation, but also relieve immune suppression within the tumor microenvironment. As YAP functions as a master regulator of many soluble factors that inhibit the anti-tumor immune response, inhibition of YAP is expected to circumvent the redundancy issues that limit the efficacy of inhibitors that target individual cytokines or receptors. By alleviating MDSC and TAM mediated immune suppression, inhibition of YAP may also enhance the effectiveness of T-cell checkpoint inhibitors, which in contrast to other solid tumors, have had limited clinical activity in pancreatic cancer (Calabro et al 2013, Le et al 2013, Royal et al 2010).

METHODS

Animals

Genetically engineered mouse strains *Yap*$^{flox/flox}$, LSL-*Kras*^{G12D}, LSL-*Trp53*^{R172H}, and *p48-Cre* were interbred to generate all experimental cohorts as described previously (Johnson et al 2001, Kawaguchi et al 2002, Olive et al 2004, Zhang et al 2014). All animal experiments were conducted in compliance with ethical regulations according to protocol #14-052 approved by the Institutional Animal Care and Use Committee at Georgetown University. Acute pancreatitis was induced in 2-month-old mice by injecting caerulein (50 mg/kg) 6 times with 1-hour intervals via i.p for two consecutive days. At 2 days, 1 week, and 5 weeks after the first injection, the mice were euthanized and the entire pancreas was dissected and processed for RNA and protein extractions, or fixing in 10% formalin. At least three mice were used for each time point for each genotype. Both males and females were included in the study without blinding or randomization.

In vivo MDSC depletion assay

2-month-old KC mice were injected with Gr1 antibody or control rat IgG (BioXCell, West Lebanon, NH; 250 μg/mouse) via i.p. injection for three days prior to initiation of caerulein treatment, after which injections with Gr1 antibody or rat IgG control were performed twice per week for two weeks in total.

Cytokine profiling

At one week post caerulein injections, WT, KPC, and KPYC mice were euthanized and the pancreas was extracted in PBS+0.5%Tween+protease inhibitor cocktail (Roche) and normalized to 5 mg/ml final concentration. Condition media (CM) from KPC and KPYC lines were collected after cultured in their respective growth medium for 48 h. All samples were stored in −80°C and shipped on dry ice to Eve Technologies (Calgary, Alberta, Canada) for Mouse Cytokine Array/Chemokine Array 31-Plex discovery assay. At least three biological repeats were included for each genotype or cell type.

Flow cytometry and immune cell isolation

Pancreata and spleens were harvested at indicated time points and mechanically disrupted in RPMI. Pancreata were then subjected to enzymatic digestion using RPMI + 10%FBS + 3.6 mg/mL collagenase D (Roche, Basel, Switzerland). Red blood cells from both pancreata and spleens were lysed using red blood cell lysing solution (eBioscience) and the resultant suspension was filtered using a 70-μm cell strainer to remove any resultant debris. Cells were then stained for intracellular and surface antigens as previously described (Surana et al 2014). The following antibodies were used for surface antigen staining:CD45 (Biolegend; clone 30-F11), CD4 (eBioscience; clone RM4-5), CD8a (Biolegend; clone 53-6.7), CD3 (Biolegend; clone 145-2C11), F4/80 (Biolegend; clone BM8), MHCII (Biolegend; cloneM5/114.15.2), Gr1(Biolegend; clone RB6-8C5), CD11b (Biolegend; clone M1/70), CD11c (Biolegend; clone N418), CD19 (BD Bioscience; clone1D3). In order to isolate $CD45^+CD3^+CD8^+$ CTLs and $CD45^+CD3^-F4/80^+$ macrophages, $CD45^+$ leukocytes were first divided into $CD3^+$ or $CD3^-$ fractions, and the $CD8^+CD4^-$ subpopulation among

$CD45^+CD3^+$ cells and the $F4/80^+$ subpopulation within $CD45^+CD3^-$ cells were collected using BD FACSAria II (BD Biosciences).

qRT-PCR

Total mRNA was purified from isolated immune cells or KPC/KPYC cells with RNAeasy Mini and micro kit (Qiagen, Hilden, Germany) according to the manufacturer's instructions. Reverse transcription was performed with iScript cDNA Synthesis Kit (Bio-Rad, Hercules, CA) and the resultant cDNA products were amplified using iTaq Universal SYBR Green Supermix (Bio-Rad) in triplicates. Relative gene expression was calculated as a unit value of $2^{-\Delta Ct}=2^{-[Ct(HPRT)-Ct(Gene\ of\ Interest))]}$. Data is represented by mean of all replicates within the genotypes. Primer sequences of the genes analyzed are listed in Table S1.

IHC/IF

IHC was performed with formalin-fixed and paraffin-embedded mouse pancreas sections as previously described (Zhang et al 2014). IF was performed after blocking in appropriate serum, followed by incubation overnight with primary antibodies at 4°C. Next day, slides were washed and incubated with HRP- or fluorescein-conjugated secondary antibodies for 30 min, and in the case when HRP-conjugated secondary antibodies were used, subjected to signal amplification with Tyramide signal amplification detection kits (Thermo Fisher Scientific) according to the manufactures' instruction. The slides were incubated with Sudan black (AMRESCO, Solon, OH) for 5 min to suppress autofluorescence and then mounted by mounting solution containing Hoechst33342. Confocal fluorescent images were obtained by a Zeiss LSM 510 Meta confocal microscope and processed with Image J software. All the quantification of signal intensity or area from IHC and IF was performed with ImageJ and data from at least 5 slides/fields were averaged. The following antibodies were used for IHC and IF: CK19 (DHSB, Iowa City, IA), Vimentin (Abcam, Cambridge, UK), αSMA (Abcam), Cleaved Caspase 3 (Cell signaling Technology, Danvers, MA), CD3 (Dako, Denmark, Glostrup, Denmark), CD45 (BD Biosciences, Franklin Lakes, NJ), CD44 (BioLegend), GZMB (Abcam), MHCII (Biolegend, San Diego, CA), F4/80 (eBioscience, San Diego, CA), Gr1 (Vio X cell), Ly6G (BD Biosciences), Ly6C (Abcam).

Cell culture

KPC/vector and KPYC/Flag-Yap lines were established previously and cultured on collagen-coated plates in Waymouth MB 752/1 Medium (Sigma-Aldrich, St. Louis, MO) containing 10% FBS (Zhang et al 2014). KPC cells established from a KPC PDAC tumor were stably transduced with pTRIPZ or pTRIPZ-Yapsh and maintained in DMEM medium (Corning, Corning, NY) containing 10% fetal bovine serum (FBS). Yapsh expression was induced by treating the cells with Doxcycline (4 μg/mL) for 3 days. Regularly mycoplasma testing was performed in house using Mycoplasma Detection Kit (InvivoGen, San Diego, CA).

In vitro MDSC differentiation and survival assay

WT mice were sacrificed by CO2 inhalation and femurs were collected. Bone marrow cells were flushed out with PBS and passed through a 28 G needle. The obtained cells were either first subjected to FACS sorting of $CD45^+CD11b^+Gr1^+$ cells or directly resuspended in

condition medium (CM) or control medium. After 5 days of incubation, cells were collected and analyzed by flow cytometry to determine the percentages of $CD11b^{+}Gr1^{+}$ MDSCs, $CD11b^{+}F4/80^{+}$ macrophages, or $CD11b^{-}CD11c^{+}$ dendritic cells within the $CD45^{+}$ population.

Western blotting

Cells were lysed with urea buffer (9.5 M urea, 2% CHAPS). Aliquots of cell lysates were heated at 95°C for 5 min and subjected to SDS-polyacrylamide gel electrophoresis. The following primary and secondary antibodies were used anti-Yap antibody (Cell Signaling), anti-actin (Santa Cruz Biotechnology), anti-rabbit IgG conjugated with horseradish peroxidase (Cell Signaling Technology), and anti-mouse IgG conjugated with horseradish peroxidase (Cell Signaling Technology)

Chromatin immunoprecipitation (ChIP)

ChIP analysis was performed as previously described using normal rabbit IgG (Santa Cruz Biotechnology, Santa Cruz, CA; Sc-2027X), antibodies against Yap (Santa Cruz Biotechnology, Sc-15407X) and Pol II (Santa Cruz Biotechnology, Sc-899X)(Zhang et al 2014). Immunoprecipitated DNA was eluted and amplified using qRT-PCR with primer pairs flanking different promoter regions of the mouse *Lif, Il6, Csf1, Csf2* and *Csf3* genes that contain putative Tead-binding sites. The primer sequences used in the study are listed in Table S1.

Microarray analysis

Snap-frozen pancreas tissues were grounded and total mRNAs were isolated using RNeasy mini kits (Qiagen). mRNA samples that passed quality check were amplified, labeled, and hybridized to Illumina MouseRef-8 v2.0 Expression BeadChips at the UCLA Neuroscience Genomics Core (Los Angeles, California). Intensity data was background corrected and normalized, and unsupervised clustering was performed in R using the *limma* package from Bioconductor. The GSEA Java-based software package from The Broad Institute was used to determine enrichment scores, significance of enrichment, and to generate enrichment plots.

TCGA analysis

The TCGA PDAC RNAseq V2 data set and associated clinical data was downloaded and processed in R. Samples were filtered to only those that were derived from tumor, based on TCGA barcoding. A group of 40 MDSC-related genes based on published literature were used to perform hierarchical clustering (Ward) on the Manhattan distance matrix between all filtered samples. The produced clustering was cut based on observable grouping. Samples with associated clinical data were used to produce survival curves in R/Prism using the R *survival* package. Only samples with overall survival >30 days were used to minimize effects from surgeries.

Statistical analysis

Minimum of three mice or independent samples were used for all the experiments unless otherwise indicated. All experiments shown were replicated at least three time or in three unique samples. Student's t-test was used to determine significance unless otherwise indicated. Significance is defined as a p value of 0.05 or less. Error bars on all graphs are standard error of the mean or standard deviation as indicated.

Supplementary Material

Refer to Web version on PubMed Central for supplementary material.

Acknowledgments

We thank Drs. T Jacks (MIT), DJ Pan (Johns Hopkins), and CV Wright (Vanderbilt) for producing and sharing the original mouse strains used in this study. We are grateful for the helpful suggestions and critical comments of our manuscript from Dr. S Ostrand-Rosenberg (UMBC). We would also like to thank Dr. Karen Creswell from the Flow Cytometry and Cell Sorting Shared Resource (FCSR) for her technical guidance. We appreciate the technical assistance from FCSR, Microscopy & Imaging Shared Resource (MISR), Histopathology & Tissue Shared Resource (HTSR), and Genomics & Epigenomics Shared Resource (GESR) at Lombardi Cancer Center Shared Resources. We thank the husbandry staff and technicians of the Division of Comparative Medicine (DCM) at Georgetown University for support in our animal studies.

Funding: C Yi is supported by NIH (R01CA187090), the V foundation, and the Advocure foundation. LM Weiner is the PI of NIH (R01CA50633), and Cancer Center Support Grant (CA051008) that also supports the Lombardi Cancer Center Shared Resources.

REFERENCES

Acharyya S, Oskarsson T, Vanharanta S, Malladi S, Kim J, Morris PG, et al. A CXCL1 paracrine network links cancer chemoresistance and metastasis. Cell. 2012; 150:165–178. [PubMed: 22770218]

Aguirre AJ, Bardeesy N, Sinha M, Lopez L, Tuveson DA, Horner J, et al. Activated Kras and Ink4a/Arf deficiency cooperate to produce metastatic pancreatic ductal adenocarcinoma. Genes Dev. 2003; 17:3112–3126. [PubMed: 14681207]

Alderson MR, Tough TW, Ziegler SF, Grabstein KH. Interleukin 7 induces cytokine secretion and tumoricidal activity by human peripheral blood monocytes. J Exp Med. 1991; 173:923–930. [PubMed: 2007858]

Bardeesy N, Sharpless NE, DePinho RA, Merlino G. The genetics of pancreatic adenocarcinoma: a roadmap for a mouse model. Semin Cancer Biol. 2001; 11:201–218. [PubMed: 11407945]

Bayne LJ, Beatty GL, Jhala N, Clark CE, Rhim AD, Stanger BZ, et al. Tumor-derived granulocyte-macrophage colony-stimulating factor regulates myeloid inflammation and T cell immunity in pancreatic cancer. Cancer Cell. 2012; 21:822–835. [PubMed: 22698406]

Bhatia M. Apoptosis versus necrosis in acute pancreatitis. Am J Physiol Gastrointest Liver Physiol. 2004; 286:G189–G196. [PubMed: 14715516]

Brembeck FH, Schreiber FS, Deramaudt TB, Craig L, Rhoades B, Swain G, et al. The mutant K-ras oncogene causes pancreatic periductal lymphocytic infiltration and gastric mucous neck cell hyperplasia in transgenic mice. Cancer Res. 2003; 63:2005–2009. [PubMed: 12727809]

Calabro L, Morra A, Fonsatti E, Cutaia O, Amato G, Giannarelli D, et al. Tremelimumab for patients with chemotherapy-resistant advanced malignant mesothelioma: an open-label, single-arm, phase 2 trial. The Lancet Oncology. 2013; 14:1104–1111. [PubMed: 24035405]

Carriere C, Young AL, Gunn JR, Longnecker DS, Korc M. Acute pancreatitis markedly accelerates pancreatic cancer progression in mice expressing oncogenic Kras. Biochem Biophys Res Commun. 2009; 382:561–565. [PubMed: 19292977]

Carriere C, Young AL, Gunn JR, Longnecker DS, Korc M. Acute pancreatitis accelerates initiation and progression to pancreatic cancer in mice expressing oncogenic Kras in the nestin cell lineage. PLoS One. 2011; 6:e27725. [PubMed: 22140463]

Clark CE, Hingorani SR, Mick R, Combs C, Tuveson DA, Vonderheide RH. Dynamics of the immune reaction to pancreatic cancer from inception to invasion. Cancer Res. 2007; 67:9518–9527. [PubMed: 17909062]

Fahey TJ 3rd, Tracey KJ, Tekamp-Olson P, Cousens LS, Jones WG, Shires GT, et al. Macrophage inflammatory protein 1 modulates macrophage function. J Immunol. 1992; 148:2764–2769. [PubMed: 1573267]

Falk LA, Vogel SN. Comparison of bone marrow progenitors responsive to granulocyte-macrophage colony stimulating factor and macrophage colony stimulating factor-1. J Leukoc Biol. 1988; 43:148–157. [PubMed: 2447217]

Feig C, Gopinathan A, Neesse A, Chan DS, Cook N, Tuveson DA. The pancreas cancer microenvironment. Clin Cancer Res. 2012; 18:4266–4276. [PubMed: 22896693]

Gabitass RF, Annels NE, Stocken DD, Pandha HA, Middleton GW. Elevated myeloid-derived suppressor cells in pancreatic, esophageal and gastric cancer are an independent prognostic factor and are associated with significant elevation of the Th2 cytokine interleukin-13. Cancer Immunol Immunother. 2011; 60:1419–1430. [PubMed: 21644036]

Grippo PJ, Nowlin PS, Demeure MJ, Longnecker DS, Sandgren EP. Preinvasive pancreatic neoplasia of ductal phenotype induced by acinar cell targeting of mutant Kras in transgenic mice. Cancer Res. 2003; 63:2016–2019. [PubMed: 12727811]

Hingorani SR, Petricoin EF, Maitra A, Rajapakse V, King C, Jacobetz MA, et al. Preinvasive and invasive ductal pancreatic cancer and its early detection in the mouse. Cancer Cell. 2003; 4:437–450. [PubMed: 14706336]

Hingorani SR, Wang L, Multani AS, Combs C, Deramaudt TB, Hruban RH, et al. Trp53R172H and KrasG12D cooperate to promote chromosomal instability and widely metastatic pancreatic ductal adenocarcinoma in mice. Cancer cell. 2005; 7:469–483. [PubMed: 15894267]

Hruban RH, Adsay NV, Albores-Saavedra J, Compton C, Garrett ES, Goodman SN, et al. Pancreatic intraepithelial neoplasia: a new nomenclature and classification system for pancreatic duct lesions. Am J Surg Pathol. 2001; 25:579–586. [PubMed: 11342768]

Hugo W, Shi H, Sun L, Piva M, Song C, Kong X, et al. Non-genomic and Immune Evolution of Melanoma Acquiring MAPKi Resistance. Cell. 2015; 162:1271–1285. [PubMed: 26359985]

Jaffee EM, Hruban RH, Canto M, Kern SE. Focus on pancreas cancer. Cancer Cell. 2002; 2:25–28. [PubMed: 12150822]

Jensen JN, Cameron E, Garay MV, Starkey TW, Gianani R, Jensen J. Recapitulation of elements of embryonic development in adult mouse pancreatic regeneration. Gastroenterology. 2005; 128:728–741. [PubMed: 15765408]

Johnson L, Mercer K, Greenbaum D, Bronson RT, Crowley D, Tuveson DA, et al. Somatic activation of the K-ras oncogene causes early onset lung cancer in mice. Nature. 2001; 410:1111–1116. [PubMed: 11323676]

Johnson R, Halder G. The two faces of Hippo: targeting the Hippo pathway for regenerative medicine and cancer treatment. Nat Rev Drug Discov. 2014; 13:63–79. [PubMed: 24336504]

Kapoor A, Yao W, Ying H, Hua S, Liewen A, Wang Q, et al. Yap1 activation enables bypass of oncogenic Kras addiction in pancreatic cancer. Cell. 2014; 158:185–197. [PubMed: 24954535]

Katoh H, Watanabe M. Myeloid-Derived Suppressor Cells and Therapeutic Strategies in Cancer. Mediators Inflamm. 2015; 2015:159269. [PubMed: 26078490]

Kawaguchi Y, Cooper B, Gannon M, Ray M, MacDonald RJ, Wright CV. The role of the transcriptional regulator Ptf1a in converting intestinal to pancreatic progenitors. Nat Genet. 2002; 32:128–134. [PubMed: 12185368]

Khaled YS, Ammori BJ, Elkord E. Increased levels of granulocytic myeloid-derived suppressor cells in peripheral blood and tumour tissue of pancreatic cancer patients. J Immunol Res. 2014; 2014:879897. [PubMed: 24741628]

Kim MH, Kim J, Hong H, Lee SH, Lee JK, Jung E. Actin remodeling confers BRAF inhibitor resistance to melanoma cells through YAP/TAZ activation. Embo J. 2015

Kitamura T, Qian BZ, Soong D, Cassetta L, Noy R, Sugano G, et al. CCL2-induced chemokine cascade promotes breast cancer metastasis by enhancing retention of metastasis-associated macrophages. J Exp Med. 2015; 212:1043–1059. [PubMed: 26056232]

Kurahara H, Takao S, Maemura K, Mataki Y, Kuwahata T, Maeda K, et al. M2-polarized tumor-associated macrophage infiltration of regional lymph nodes is associated with nodal lymphangiogenesis and occult nodal involvement in pN0 pancreatic cancer. Pancreas. 2013; 42:155–159. [PubMed: 22699204]

Lacey DC, Achuthan A, Fleetwood AJ, Dinh H, Roiniotis J, Scholz GM, et al. Defining GM-CSF- and macrophage-CSF-dependent macrophage responses by in vitro models. J Immunol. 2012; 188:5752–5765. [PubMed: 22547697]

Le DT, Lutz E, Uram JN, Sugar EA, Onners B, Solt S, et al. Evaluation of ipilimumab in combination with allogeneic pancreatic tumor cells transfected with a GM-CSF gene in previously treated pancreatic cancer. J Immunother. 2013; 36:382–389. [PubMed: 23924790]

Lechner MG, Liebertz DJ, Epstein AL. Characterization of cytokine-induced myeloid-derived suppressor cells from normal human peripheral blood mononuclear cells. J Immunol. 2010; 185:2273–2284. [PubMed: 20644162]

Li X, Yao W, Yuan Y, Chen P, Li B, Li J, et al. Targeting of tumour-infiltrating macrophages via CCL2/CCR2 signalling as a therapeutic strategy against hepatocellular carcinoma. Gut. 2015

Lin L, Sabnis AJ, Chan E, Olivas V, Cade L, Pazarentzos E, et al. The Hippo effector YAP promotes resistance to RAF- and MEK-targeted cancer therapies. Nat Genet. 2015; 47:250–256. [PubMed: 25665005]

Lindell DM, Standiford TJ, Mancuso P, Leshen ZJ, Huffnagle GB. Macrophage inflammatory protein 1alpha/CCL3 is required for clearance of an acute Klebsiella pneumoniae pulmonary infection. Infect Immun. 2001; 69:6364–6369. [PubMed: 11553580]

Lowenfels AB, Maisonneuve P, Cavallini G, Ammann RW, Lankisch PG, Andersen JR, et al. Pancreatitis and the risk of pancreatic cancer. International Pancreatitis Study Group. N Engl J Med. 1993; 328:1433–1437. [PubMed: 8479461]

Lu T, Ramakrishnan R, Altiok S, Youn JI, Cheng P, Celis E, et al. Tumor-infiltrating myeloid cells induce tumor cell resistance to cytotoxic T cells in mice. J Clin Invest. 2011; 121:4015–4029. [PubMed: 21911941]

Mace TA, Ameen Z, Collins A, Wojcik S, Mair M, Young GS, et al. Pancreatic cancer-associated stellate cells promote differentiation of myeloid-derived suppressor cells in a STAT3-dependent manner. Cancer Res. 2013; 73:3007–3018. [PubMed: 23514705]

Marigo I, Bosio E, Solito S, Mesa C, Fernandez A, Dolcetti L, et al. Tumor-induced tolerance and immune suppression depend on the C/EBPbeta transcription factor. Immunity. 2010; 32:790–802. [PubMed: 20605485]

Markowitz J, Brooks TR, Duggan MC, Paul BK, Pan X, Wei L, et al. Patients with pancreatic adenocarcinoma exhibit elevated levels of myeloid-derived suppressor cells upon progression of disease. Cancer Immunol Immunother. 2015; 64:149–159. [PubMed: 25305035]

Mok S, Koya RC, Tsui C, Xu J, Robert L, Wu L, et al. Inhibition of CSF-1 receptor improves the antitumor efficacy of adoptive cell transfer immunotherapy. Cancer Res. 2014; 74:153–161. [PubMed: 24247719]

Morris, JPt, Cano, DA., Sekine, S., Wang, SC., Hebrok, M. Beta-catenin blocks Kras-dependent reprogramming of acini into pancreatic cancer precursor lesions in mice. J Clin Invest. 2010; 120:508–520. [PubMed: 20071774]

Munigala S, Kanwal F, Xian H, Scherrer JF, Agarwal B. Increased risk of pancreatic adenocarcinoma after acute pancreatitis. Clin Gastroenterol Hepatol. 2014; 12:1143–1150. e1141. [PubMed: 24440214]

Noy R, Pollard JW. Tumor-associated macrophages: from mechanisms to therapy. Immunity. 2014; 41:49–61. [PubMed: 25035953]

Obermajer N, Muthuswamy R, Odunsi K, Edwards RP, Kalinski P. PGE(2)-induced CXCL12 production and CXCR4 expression controls the accumulation of human MDSCs in ovarian cancer environment. Cancer Res. 2011; 71:7463–7470. [PubMed: 22025564]

Obermajer N, Wong JL, Edwards RP, Odunsi K, Moysich K, Kalinski P. PGE(2)-driven induction and maintenance of cancer-associated myeloid-derived suppressor cells. Immunol Invest. 2012; 41:635–657. [PubMed: 23017139]

Olive KP, Tuveson DA, Ruhe ZC, Yin B, Willis NA, Bronson RT, et al. Mutant p53 gain of function in two mouse models of Li-Fraumeni syndrome. Cell. 2004; 119:847–860. [PubMed: 15607980]

Parker KH, Beury DW, Ostrand-Rosenberg S. Myeloid-Derived Suppressor Cells: Critical Cells Driving Immune Suppression in the Tumor Microenvironment. Adv Cancer Res. 2015; 128:95–139. [PubMed: 26216631]

Phan VT, Wu X, Cheng JH, Sheng RX, Chung AS, Zhuang G, et al. Oncogenic RAS pathway activation promotes resistance to anti-VEGF therapy through G-CSF-induced neutrophil recruitment. Proc Natl Acad Sci U S A. 2013; 110:6079–6084. [PubMed: 23530240]

Plouffe SW, Hong AW, Guan KL. Disease implications of the Hippo/YAP pathway. Trends Mol Med. 2015; 21:212–222. [PubMed: 25702974]

Porembka MR, Mitchem JB, Belt BA, Hsieh CS, Lee HM, Herndon J, et al. Pancreatic adenocarcinoma induces bone marrow mobilization of myeloid-derived suppressor cells which promote primary tumor growth. Cancer Immunol Immunother. 2012; 61:1373–1385. [PubMed: 22215137]

Pylayeva-Gupta Y, Lee KE, Hajdu CH, Miller G, Bar-Sagi D. Oncogenic Kras-induced GM-CSF production promotes the development of pancreatic neoplasia. Cancer Cell. 2012; 21:836–847. [PubMed: 22698407]

Roca H, Varsos ZS, Sud S, Craig MJ, Ying C, Pienta KJ. CCL2 and interleukin-6 promote survival of human CD11b+ peripheral blood mononuclear cells and induce M2-type macrophage polarization. J Biol Chem. 2009; 284:34342–34354. [PubMed: 19833726]

Royal RE, Levy C, Turner K, Mathur A, Hughes M, Kammula US, et al. Phase 2 trial of single agent Ipilimumab (anti-CTLA-4) for locally advanced or metastatic pancreatic adenocarcinoma. J Immunother. 2010; 33:828–833. [PubMed: 20842054]

Ryan DP, Hong TS, Bardeesy N. Pancreatic adenocarcinoma. N Engl J Med. 2014; 371:1039–1049. [PubMed: 25207767]

Schutte M, Hruban RH, Geradts J, Maynard R, Hilgers W, Rabindran SK, et al. Abrogation of the Rb/p16 tumor-suppressive pathway in virtually all pancreatic carcinomas. Cancer Res. 1997; 57:3126–3130. [PubMed: 9242437]

Shao DD, Xue W, Krall EB, Bhutkar A, Piccioni F, Wang X, et al. KRAS and YAP1 converge to regulate EMT and tumor survival. Cell. 2014; 158:171–184. [PubMed: 24954536]

Siegel RL, Miller KD, Jemal A. Cancer statistics, 2015. CA Cancer J Clin. 2015; 65:5–29. [PubMed: 25559415]

Sierra-Filardi E, Nieto C, Dominguez-Soto A, Barroso R, Sanchez-Mateos P, Puig-Kroger A, et al. CCL2 shapes macrophage polarization by GM-CSF and M-CSF: identification of CCL2/CCR2-dependent gene expression profile. J Immunol. 2014; 192:3858–3867. [PubMed: 24639350]

Sinha P, Clements VK, Fulton AM, Ostrand-Rosenberg S. Prostaglandin E2 promotes tumor progression by inducing myeloid-derived suppressor cells. Cancer Res. 2007; 67:4507–4513. [PubMed: 17483367]

Sinha P, Okoro C, Foell D, Freeze HH, Ostrand-Rosenberg S, Srikrishna G. Proinflammatory S100 proteins regulate the accumulation of myeloid-derived suppressor cells. J Immunol. 2008; 181:4666–4675. [PubMed: 18802069]

Strauss L, Sangaletti S, Consonni FM, Szebeni G, Morlacchi S, Totaro MG, et al. RORC1 Regulates Tumor-Promoting "Emergency" Granulo-Monocytopoiesis. Cancer Cell. 2015; 28:253–269. [PubMed: 26267538]

Stromnes IM, Brockenbrough JS, Izeradjene K, Carlson MA, Cuevas C, Simmons RM, et al. Targeted depletion of an MDSC subset unmasks pancreatic ductal adenocarcinoma to adaptive immunity. Gut. 2014; 63:1769–1781. [PubMed: 24555999]

Surana R, Wang S, Xu W, Jablonski SA, Weiner LM. IL4 limits the efficacy of tumor-targeted antibody therapy in a murine model. Cancer Immunol Res. 2014; 2:1103–1112. [PubMed: 25204776]

Tsou CL, Peters W, Si Y, Slaymaker S, Aslanian AM, Weisberg SP, et al. Critical roles for CCR2 and MCP-3 in monocyte mobilization from bone marrow and recruitment to inflammatory sites. J Clin Invest. 2007; 117:902–909. [PubMed: 17364026]

Tuveson DA, Zhu L, Gopinathan A, Willis NA, Kachatrian L, Grochow R, et al. Mist1-KrasG12D knock-in mice develop mixed differentiation metastatic exocrine pancreatic carcinoma and hepatocellular carcinoma. Cancer Res. 2006; 66:242–247. [PubMed: 16397237]

Wang G, Lu X, Dey P, Deng P, Wu CC, Jiang S, et al. Targeting YAP-Dependent MDSC Infiltration Impairs Tumor Progression. Cancer Discov. 2016; 6:80–95. [PubMed: 26701088]

Xue J, Sharma V, Hsieh MH, Chawla A, Murali R, Pandol SJ, et al. Alternatively activated macrophages promote pancreatic fibrosis in chronic pancreatitis. Nat Commun. 2015; 6:7158. [PubMed: 25981357]

Zeng L, Guo Y, Liang J, Chen S, Peng P, Zhang Q, et al. Perineural Invasion and TAMs in Pancreatic Ductal Adenocarcinomas: Review of the Original Pathology Reports Using Immunohistochemical Enhancement and Relationships with Clinicopathological Features. J Cancer. 2014; 5:754–760. [PubMed: 25368675]

Zhang W, Nandakumar N, Shi Y, Manzano M, Smith A, Graham G, et al. Downstream of mutant KRAS, the transcription regulator YAP is essential for neoplastic progression to pancreatic ductal adenocarcinoma. Sci Signal. 2014; 7:ra42. [PubMed: 24803537]

Zhang Y, Liu Q, Zhang M, Yu Y, Liu X, Cao X. Fas signal promotes lung cancer growth by recruiting myeloid-derived suppressor cells via cancer cell-derived PGE2. J Immunol. 2009; 182:3801–3808. [PubMed: 19265159]

Zhao F, Obermann S, von Wasielewski R, Haile L, Manns MP, Korangy F, et al. Increase in frequency of myeloid-derived suppressor cells in mice with spontaneous pancreatic carcinoma. Immunology. 2009; 128:141–149. [PubMed: 19689743]

Zhao X, Rong L, Li X, Liu X, Deng J, Wu H, et al. TNF signaling drives myeloid-derived suppressor cell accumulation. J Clin Invest. 2012; 122:4094–4104. [PubMed: 23064360]

Zhu Y, Knolhoff BL, Meyer MA, Nywening TM, West BL, Luo J, et al. CSF1/CSF1R Blockade Reprograms Tumor-Infiltrating Macrophages and Improves Response to T-cell Checkpoint Immunotherapy in Pancreatic Cancer Models. Cancer Res. 2014; 74:5057–5069. [PubMed: 25082815]

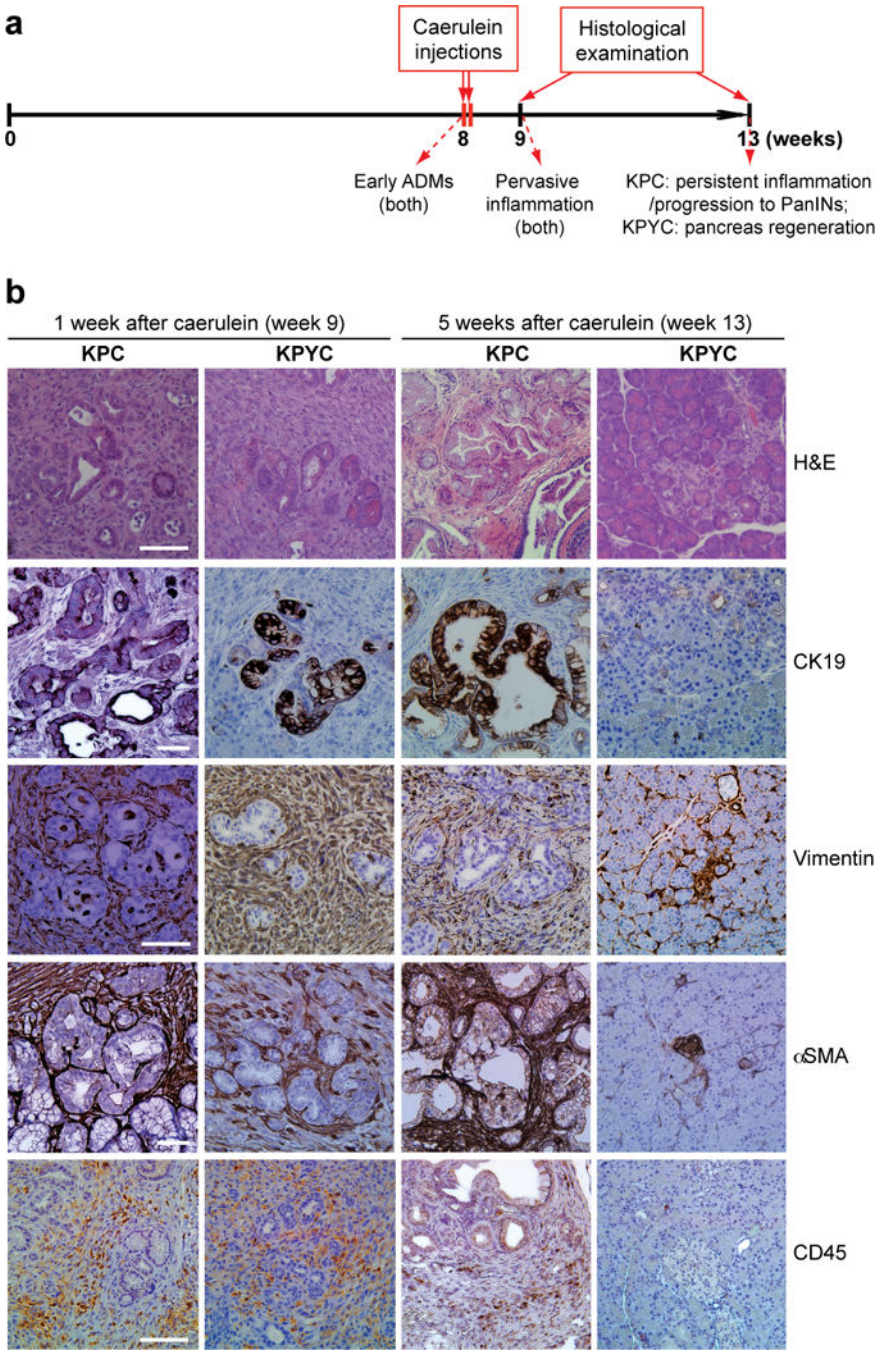

Figure 1. Deletion of *Yap* in *Kras:p53* mutant pancreata results in tissue regeneration following acute pancreatitis

(a) Experimental design and summary of phenotypes at the indicated time points.

(b) Representative images of H&E, CK19, Vimentin, αSMA, and CD45 IHC staining of pancreas sections from KPC and KPYC mice at 1 week or 5 weeks post caerulein injections. Scale bar indicates 200 μm.

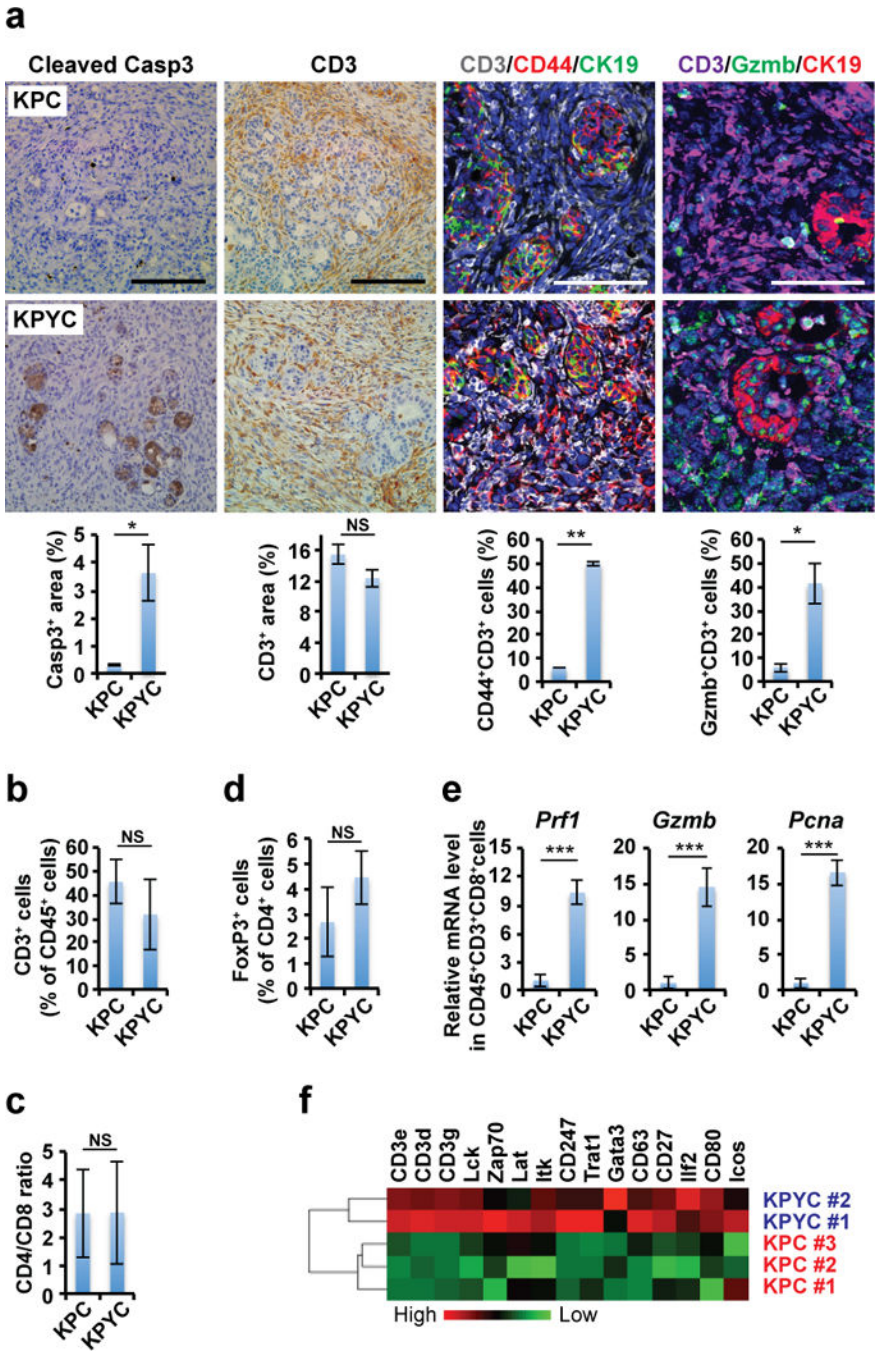

Figure 2. Deletion of *Yap* reactivates T cells and promotes *Kras:Trp53* mutant neoplastic ducts to undergo apoptosis following acute pancreatitis

(a) Representative images and quantification of the percentage of cleaved-Caspase 3 (cleaved Casp3) and CD3 IHC staining, and IF staining for CD3/CD44/CK19 and CD3/Gzmb/CK19 in the pancreas sections from KPC and KPYC mice at 1 week post caerulein injections. Error bars represent standard errors. Scale bar indicates 200 μm. *P<0.05; **P<0.005; NS: not significant.

(b) Percentage of $CD3^+$ T cells among total $CD45^+$ leukocytes in pancreata from 9-week-old KPC (n = 6) and KPYC (n = 3) mice at 1 week post caerulein injections as determined by flow cytometry. Error bars indicate standard deviations. NS: not significant.

(c) Ratio of CD4/CD8 positive cells in the pancreata of 9-week-old KPC (n = 7) and KPYC (n = 3) mice at 1 week post caerulein injections as determined by flow cytometry. Error bars indicate standard deviations. NS: not significant.

(d) Percentage of $CD4^+FoxP3^+$ regulatory T cells among total $CD4^+$ leukocytes in pancreata from 9-week-old KPC (n = 4) and KPYC (n = 3) mice at 1 week post caerulein injections as determined by flow cytometry. Error bars indicate standard deviations. NS: not significant.

(e) Relative mRNA expression of *Prf1*, *Gzmb*, and *Pcna* in $CD45^+CD3^+CD8^+$ cytotoxic T cells isolated from pancreata of 9-week-old KPC (n = 3) and KPYC (n= 4) mice at 1 week post caerulein challenge as determined by qRT-PCR. Error bars indicate standard errors. ***P<0.0005.

(f) Heatmap of relative mRNA expression of genes involved in TCR signaling in pancreata from 9-week-old KPC and KPYC mice at 1 week post caerulein injections as determined by microarray analysis.

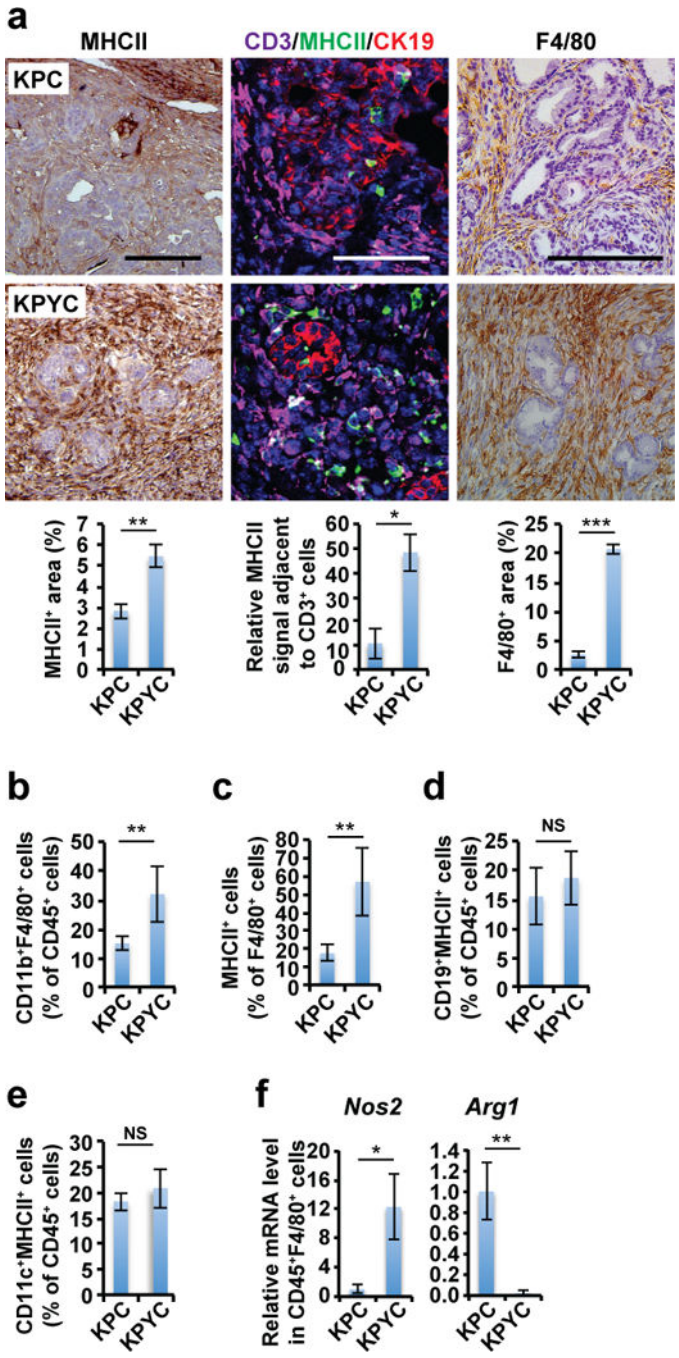

Figure 3. Depletion of *Yap* enhances infiltration of MHCII^{+} macrophages in *Kras:Trp53* mutant pancreata following acute pancreatitis

(a) Representative images and quantification of the percentage of MHCII and F4/80 IHC staining, and CD3, MHCII and CK19 IF signal intensity in pancreatic sections from 9-week-old KPC and KPYC mice at 1 week post caerulein injections. Error bars indicate standard errors. Scale bar indicates 200 μm. *P<0.05; **P<0.005; ***P<0.0005.

(b) Percentage of $CD11b^+F4/80^+$ macrophages among total $CD45^+$ leukocytes in pancreata from 9-week-old KPC (n = 6) and KPYC (n = 5) mice at 1 week post caerulein injections as determined by flow cytometry. Error bars indicate standard deviations. **P<0.005.
(c) Percentage of MHC II^+ cells among $CD45^+CD11b^+F4/80^+$ macrophages in pancreata from 9-week-old KPC (n = 5) and KPYC (n = 4) mice at 1 week post caerulein injections as determined by flow cytometry. Error bars indicate standard deviations. **P<0.005.
(d) Percentage of $CD19^+MHCII^+$ B-cells among total $CD45^+$ leukocytes in pancreata from 9-week-old KPC (n = 6) and KPYC (n = 4) mice at 1 week post caerulein injections as determined by flow cytometry. Error bars indicate standard deviations.. NS: not significant.
(e) Percentage of $CD11c^+MHCII^+$ dendritic cells among total $CD45^+$ leukocytes in pancreata from 9-week-old KPC (n = 3) and KPYC (n = 5) mice at 1 week post caerulein injections as determined by flow cytometry. Error bars indicate standard deviations.. NS: not significant.
(f) Relative mRNA expression of *Nos2* and *Arg* in $CD45^+F4/80^+$ macrophages isolated from pancreata of 9-week-old KPC (n = 3) and KPYC (n = 7) animals at 1 week post caerulein challenge as determined by qRT-PCR. Error bars indicate standard errors. *P<0.05; **P<0.005.

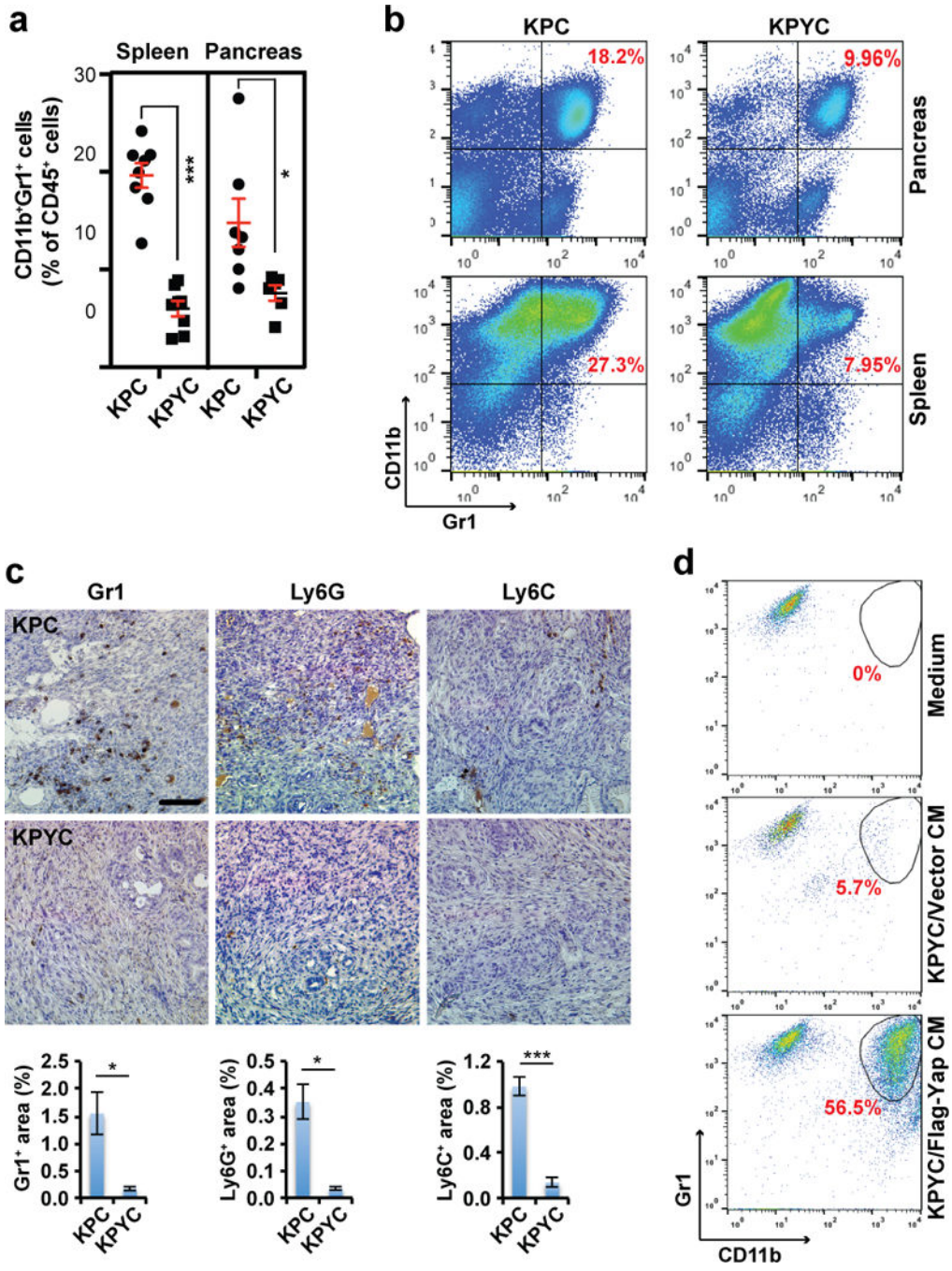

Figure 4. *Yap* knockout blocks accumulation of MDSCs in the spleen and pancreata of *Kras:Trp53* mutant mice following acute pancreatitis

(a) Percentage of of $Gr1^+CD11b^+$ MDSC cells among total $CD45^+$ leukocytes in spleens and pancreata from 9-week-old KPC (spleen, n = 8; pancreas, n = 7) and KPYC (spleen, n = 6; pancreas, n = 5) mice at 1 week post caerulein injections as determined by flow cytometry. Symbols represent data from individual mice, and bars show the mean. Error bars indicate standard deviations. *P<0.05; ***P<0.0005.

(b) Representative plots of flow cytometry analysis of $Gr1^+CD11b^+$ MDSC. The percentage of $Gr1^+CD11b^+$ cells among all CD45+ leukocytes is indicated in red.
(c) Representative images and quantification of the percentage of Gr1, Ly6C, and Ly6G IHC staining in pancreatic sections from 9-week-old KPC and KPYC mice at 1 week post caerulein challenge. Error bars indicate standard errors. Scale bar indicates 200 μm. *P<0.05; ***P<0.0005.
(d) Representative plots of flow cytometry analysis of $Gr1^+CD11b^+$ MDSC cells following 5 days of incubation of WT bone marrow cells with control medium or conditioned medium (CM) from KPYC cells transduced with vector control or Flag-Yap. The $Gr1^+CD11b^+$ population is gated and the percentage among all $CD45^+$ leukocytes is indicated in red. Error bars indicate standard errors.

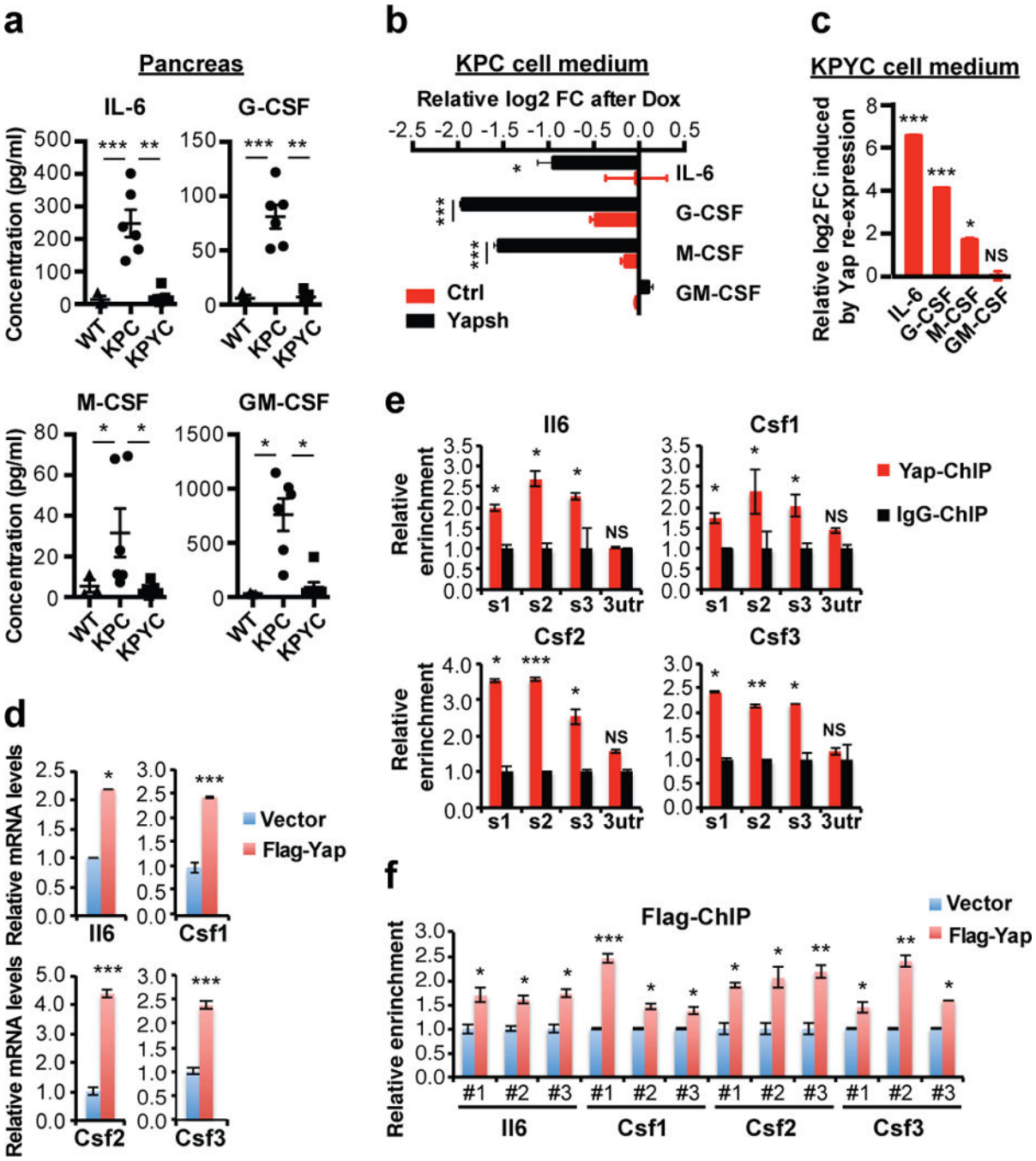

Figure 5. Silencing of Yap in *Kras:Trp53* mutant PDAC cells inhibits the transcription and secretion of MDSC-polarizing cytokines

(a) Quantification of indicated cytokines in pancreata from 9-week-old WT (n = 3), KPC (n =6), and KPYC (n = 7) mice at 1 week post caerulein injection as determined by ELISA. Symbols represent data from individual mice, and bars show the mean. Error bars indicate standard deviation. *P<0.05; **P<0.005; ***P<0.0005.

(b) Relative log2 fold changes (FC) of indicated cytokines in the conditioned media (CM) of KPC PDAC cells harboring pTRIPZ empty vector (Ctrl) or pTRIPZ-shYap (Yapsh) after addition of Dox. Error bars indicate standard deviation. *P<0.05; ***P<0.0005.

(c) Relative log2 FC of indicated cytokines in the CM from KPYC cells re-expressing Yap compared to CM from KPYC control cells. Error bars indicate standard deviation. *P<0.05; **P<0.005; NS: not significant.

(d) Relative mRNA expression of indicated genes in KPYC cells introduced with vector control or Flag-Yap as determined by qRT-PCR analysis. Error bars indicate standard error. *P<0.05; ***P<0.0005.

(e) qRT-PCR analysis of ChIP with control IgG and Yap antibodies against promoter regions containing putative Tead-binding motifs (S1-3) of indicated genes in KPC PDAC cells. The 3'UTR sequences were used as negative controls. Error bars indicate standard error. *P<0.05; **P<0.005; ***P<0.0005; NS: not significant.

(f) qRT-PCR analysis of ChIP with Flag antibodies in KPYC cells introduced with control vector or Flag-Yap using the same set of primers as in (e). Error bars indicate standard error. *P<0.05; **P<0.005; ***P<0.0005.

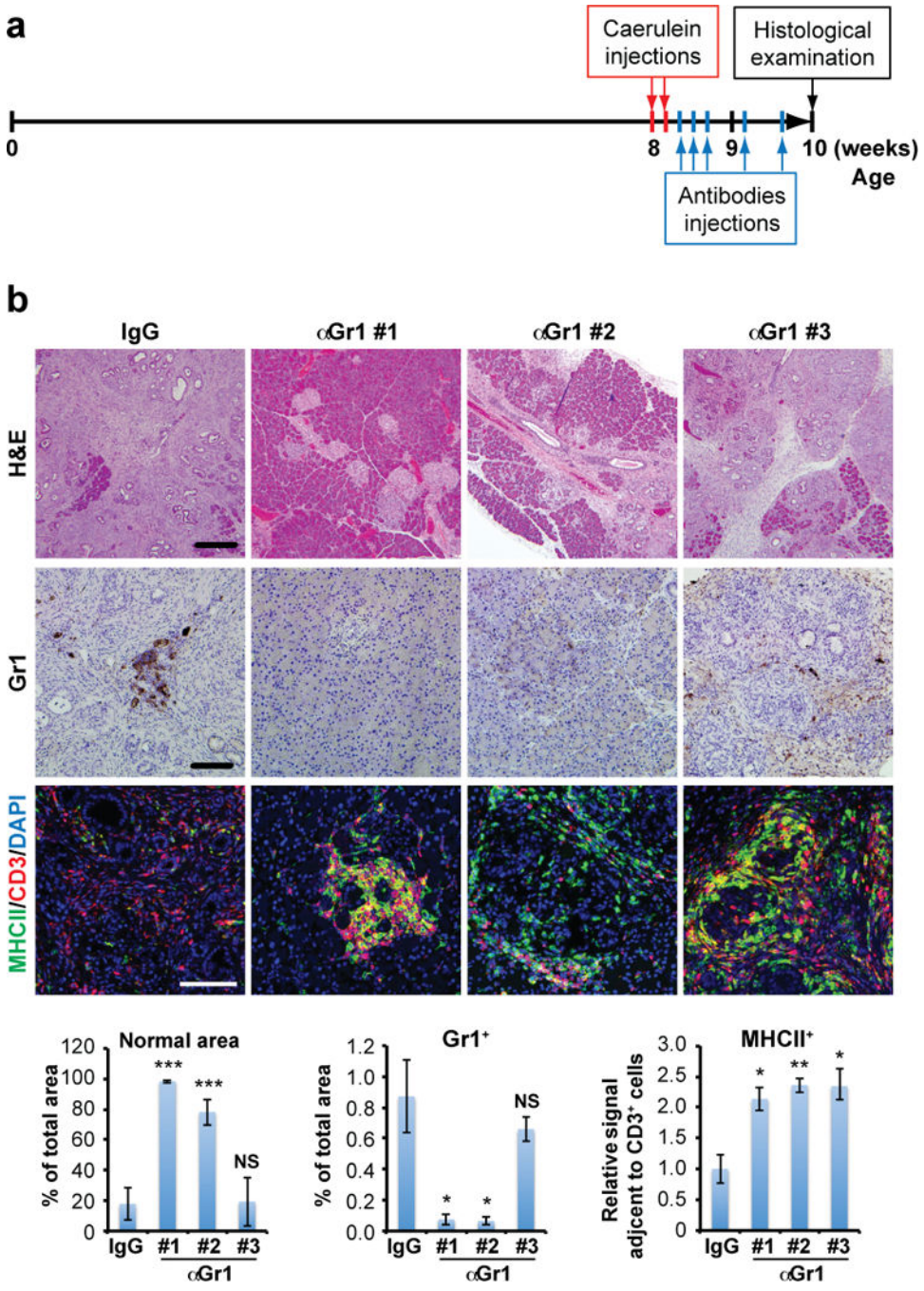

Figure 6. Depletion of MDSCs restores infiltration of MHCII$^+$ cells and promotes pancreatic regeneration in KC mice

(a) Experimental design.

(b) Representative images and quantification of H&E, Gr1 IHC, and MHCII/CD3 IF staining of pancreatic sections from 10-week-old KC mice that were subjected to caerulein and antibody injections as outlined in (a). Error bars represent standard errors. #1-3 indicate three different mice injected with αGr1 antibody. Scale bar indicates 200 μm. *P<0.05; **P<0.005; ***P<0.0005; NS: not significant.

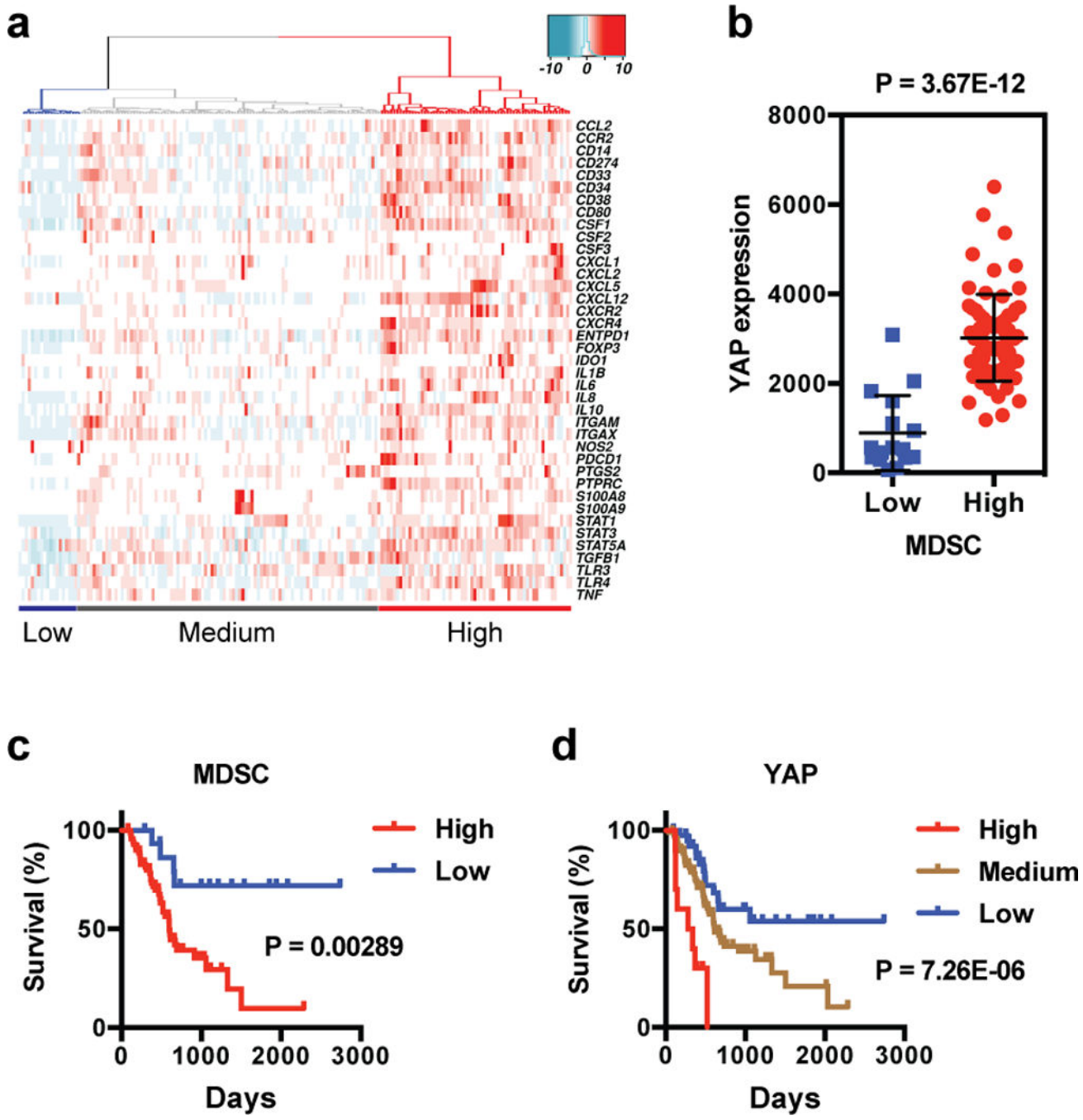

Figure 7. Yap expression correlates with expression of MDSC-related genes and predicts survival in human PDAC

(a) Heatmap of unsupervised hierarchical clustering analysis of expression of 40 MDSC-related genes in TCGA primary PDAC tumor samples with RNAseq expression information (n=179). Three major clusters are identified as “Low” (n=19), “Medium” (n=63), or “High” (n=97) .

(b) Relative *YAP* mRNA levels in TCGA primary PDAC tumors classified as either MDSC “High” or MDSC “Low” as in (a).

(c) Kaplan-Meier overall survival curve of PDAC patients with either “High” (n=71) or “Low” (n=16) MDSC expression profiles.
(d) Kaplan-Meier survival curve of PDAC patients stratified by Low (n=39), Medium (n=98), or High (n=10) relative *YAP* expression.

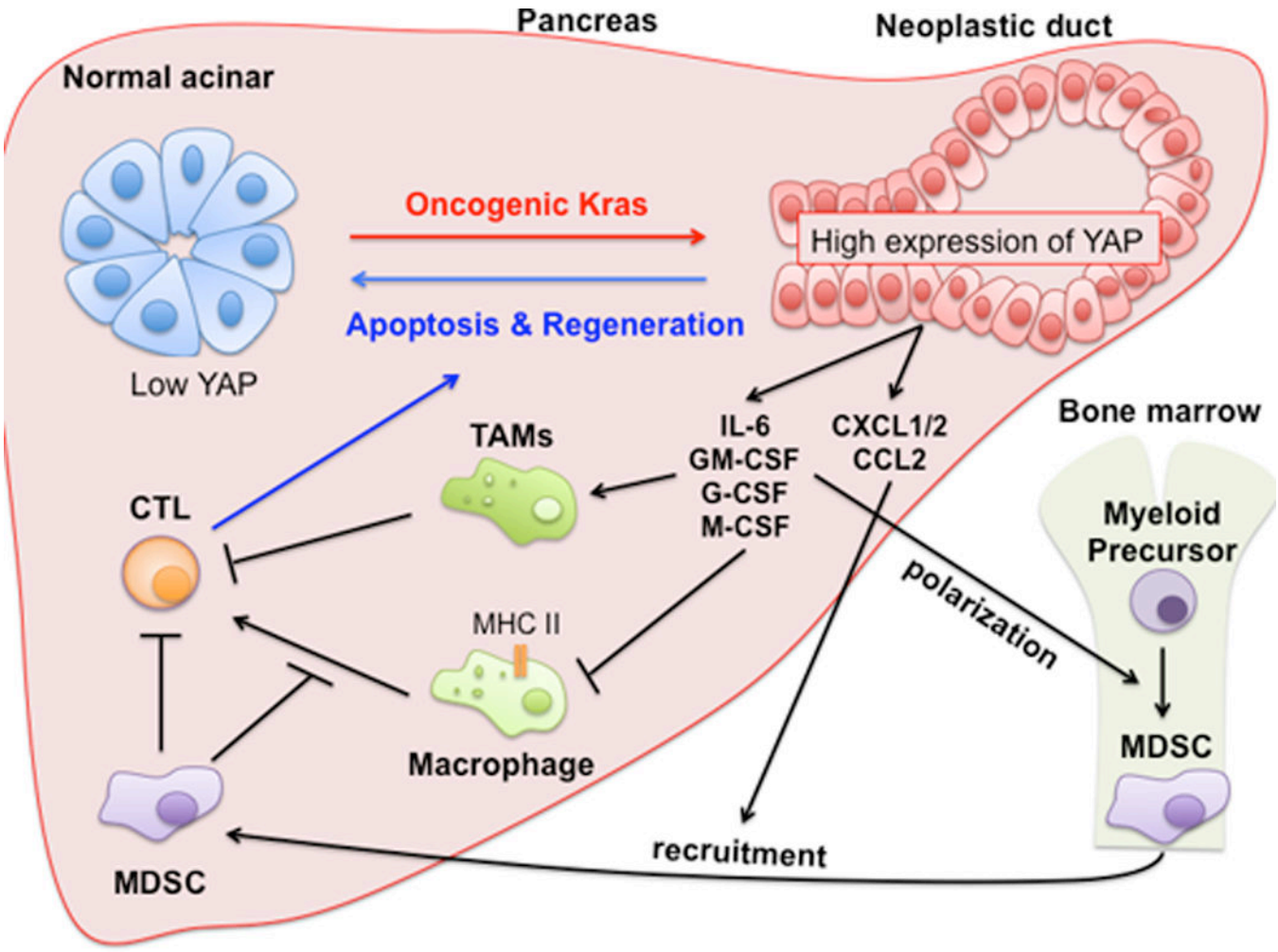

Figure 8. Yap orchestrates an immune suppressive microenvironment in *Kras* mutant pancreas by promoting the expression of MDSC-promoting cytokines

Schematic representation of the crucial function of Yap as a master switch of an ongenic Kras secretome that promotes the accumulation of immune suppressive MDSCs and TAMs and downregulates antigen-presenting macrophages, leading to suppression of CTLs.